

Search for a dark photon in the A' Experiment (APEX)

S. Abrahamyan,¹ Z. Ahmed,² K. Allada,³ D. Anez,⁴ T. Averett,⁵ A. Barbieri,⁶ K. Bartlett,⁷ J. Beacham,⁸ J. Bono,⁹ J. Boyce,¹⁰ P. Brindza,¹⁰ A. Camsonne,¹⁰ K. Cranmer,⁸ M. Dalton,⁶ C.W. de Jager,¹⁰ J. Donaghy,⁷ R. Essig,^{11,*} C. Field,¹¹ E. Folts,¹⁰ N. Goeckner-Wald,¹² J. Gomez,¹⁰ M. Graham,¹¹ J.-O. Hansen,¹⁰ D.W. Higinbotham,¹⁰ T. Holmstrom,¹³ J. Huang,¹⁴ S. Iqbal,¹⁵ J. Jaros,¹¹ E. Jensen,⁵ A. Kelleher,¹⁴ M. Khandaker,^{16,10} J. LeRose,¹⁰ R. Lindgren,⁶ N. Liyanage,⁶ E. Long,¹⁷ J. Mammei,¹⁸ P. Markowitz,⁹ T. Maruyama,¹¹ V. Maxwell,⁹ S. Mayilyan,¹ J. McDonald,¹¹ R. Michaels,¹⁰ K. Moffeit,¹¹ V. Nelyubin,⁶ A. Odian,¹¹ M. Oriunno,¹¹ R. Partridge,¹¹ M. Paolone,¹⁹ E. Piasetzky,²⁰ I. Pomerantz,²⁰ Y. Qiang,¹⁰ S. Riordan,¹⁸ Y. Roblin,¹⁰ B. Sawatzky,¹⁰ P. Schuster,^{11,21,†} J. Segal,¹⁰ L. Selvy,¹⁷ A. Shahinyan,¹ R. Subedi,²² V. Sulkosky,¹⁴ S. Stepanyan,¹⁰ N. Toro,^{23,21,‡} D. Waltz,¹¹ B. Wojtsekhowski,^{10,§} and J. Zhang¹⁰

¹Yerevan Physics Institute, Yerevan 375036, Armenia

²Syracuse University, Syracuse, New York 13244

³University of Kentucky, Lexington, Kentucky 40506

⁴Saint Mary's University, Halifax, NS B3H 3C3, Canada

⁵College of William and Mary, Williamsburg, Virginia 23187

⁶University of Virginia, Charlottesville, Virginia 22903

⁷University of New Hampshire, Durham, New Hampshire 03824

⁸New York University, New York, New York 10012

⁹Florida International University, Miami, Florida 33199

¹⁰Thomas Jefferson National Accelerator Facility, Newport News, Virginia 23606

¹¹SLAC National Accelerator Laboratory, Menlo Park, California 94025

¹²Carnegie Mellon University, Pittsburgh, Pennsylvania 15213

¹³Longwood University, Farmville, Virginia 23909

¹⁴Massachusetts Institute of Technology, Cambridge, Massachusetts 02139

¹⁵California State University at Los Angeles, Los Angeles, California 90032

¹⁶Norfolk State University, Norfolk, Virginia 23504

¹⁷Kent State University, Kent, Ohio 44242

¹⁸University of Massachusetts, Amherst, Massachusetts 01003

¹⁹University of South Carolina, Columbia, South Carolina 29225

²⁰Tel Aviv University, Tel Aviv, 69978 Israel

²¹Perimeter Institute for Theoretical Physics, Waterloo, ON N2L 2Y5, Canada

²²George Washington University, Washington DC

²³Stanford University, Menlo Park, California 94025

(Dated: July 1, 2011)

We present a search at Jefferson Lab for new forces mediated by sub-GeV vector bosons with weak coupling α' to electrons. Such a particle A' can be produced in electron-nucleus fixed-target scattering, and then decay to an e^+e^- pair, producing a narrow resonance in the QED trident spectrum. Using APEX test run data, we searched in the mass range 175–250 MeV, finding no evidence for an $A' \rightarrow e^+e^-$ reaction, and set an upper limit of $\alpha'/\alpha \simeq 10^{-6}$. Our findings demonstrate that fixed-target searches can explore a new, wide, and important range of masses and couplings for sub-GeV forces.

The strong, weak, and electromagnetic forces are mediated by vector bosons of the Standard Model. New forces could have escaped detection only if their mediators are either heavier than $\mathcal{O}(\text{TeV})$ or quite weakly coupled. The latter possibility can be tested by precision colliding-beam and fixed-target experiments. This *letter* presents the results of a search for sub-GeV mediators of weakly coupled new forces in a test run for the A' Experiment (APEX), which was proposed in [1, 2] based on ideas presented in [3].

A new $U(1)'$ gauge boson, A' , can acquire a small coupling to charged particles if it mixes kinetically with the photon [4]. Indeed, quantum loops of heavy particles with electric and $U(1)'$ charges can generate kinetic mixing and an effective coupling $\epsilon e A'_\mu J_{EM}^\mu$ of the A' to the electromagnetic current J_{EM}^μ , suppressed relative to the electron charge e by $\epsilon \sim 10^{-2} - 10^{-6}$ [5]. This mechanism motivates the search

for very weakly coupled gauge bosons. A' masses in the MeV–GeV range have received renewed interest as a possible explanation of various data anomalies related to dark matter [6, 7] and of the discrepancy between the calculated and measured anomalous magnetic moment of the muon [8]. A' 's in the same mass range arise in several theoretical proposals [9–11], and their couplings to charged matter, $\alpha' \equiv \epsilon^2 \alpha$ ($\alpha = e^2/4\pi$), are remarkably weakly constrained [3].

The simplest scenario, in which the A' decays directly to ordinary matter, can be tested in electron and proton fixed-target experiments [3, 12–14] and at e^+e^- and hadron colliders [5, 10, 15–20]. Electron fixed-target experiments are uniquely suited to probing the sub-GeV mass range because of their high luminosity, large cross-sections, and favorable kinematics. Electrons scattering off target nuclei can radiate an A' , which then decays to e^+e^- , see Fig. 1. The A' would

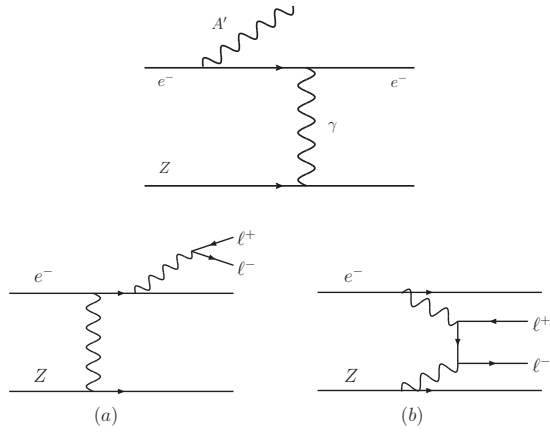


FIG. 1. Top: A' production from radiation off an incoming e^- beam incident on a target consisting of nuclei of atomic number Z . APEX is sensitive to A' decays to e^+e^- pairs, although decays to $\mu^+\mu^-$ pairs are possible for A' masses $m_{A'} > 2m_\mu$. Bottom: QED trident backgrounds: (a) radiative tridents and (b) Bethe-Heitler tridents. **will update (thicker lines)**

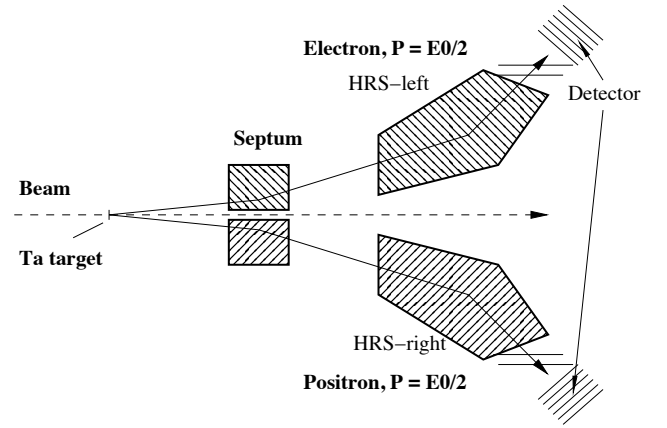


FIG. 2. The layout of the APEX test run. An electron beam (left-to-right) is incident on a thin Tantalum foil target. Two septa magnets of opposite polarity bend charged particles to larger angles into two vertical-bend high resolution spectrometers (HRS) set up to select electrons and positrons each carrying close to half the incoming beam energy. The HRS contain detectors to accurately measure the momentum, direction, and identity of the particles.

then appear as a small, narrow resonance in the e^+e^- invariant mass spectrum, over the large background from quantum electrodynamics (QED) trident processes. APEX is optimized to search for such a resonance using Jefferson Laboratory's Continuous Electron Beam Accelerator Facility and the superior mass resolution attainable with the High Resolution Spectrometers (HRS) in Hall A [21].

The full APEX experiment will probe couplings $\alpha'/\alpha \gtrsim 10^{-7}$ and masses $\sim 50 - 550$ MeV, an enormous improvement in cross section sensitivity over all previous experiments. Other electron fixed target experiments are planned at Jefferson Laboratory, including the Heavy Photon Search (HPS) [22] and DarkLight [13]; at MAMI [23]; and at DESY (the Hidden Photon Search (HIPS) [24]).

We present here the results of a test run for APEX that took place July 2010. The layout of the experiment is shown in Fig. 2. The distinctive kinematics of A' production motivates the choice of configuration. The A' typically carries a large fraction of the incident beam energy E_b , is produced forward at angles $\sim (m_{A'}/E_b)^{3/2} \ll 1$, and decays to an e^+e^- pair with a typical opening angle of $m_{A'}/E_b$. A symmetric configuration with the e^- and e^+ each carrying nearly half the beam energy mitigates QED background while maintaining high signal efficiency.

The test run used a (2.260 ± 0.002) GeV electron beam with an intensity up to $150 \mu\text{A}$ incident on a Tantalum foil of thickness 21.5 mg/cm^2 (3.15×10^{-3} radiation lengths). The central momentum was $1.131(2)$ GeV for the left (right) HRS with a momentum acceptance from 1.079 to 1.181 GeV. Dipole septum magnets between the target and the HRS aperture allow the detection of e^- 's and e^+ 's at central angles of 5° relative to the incident beam. Collimators present during the test run

reduced the solid angle acceptance of each spectrometer from a nominal 4.3 msr to $\simeq 2.8$ (2.9) msr for the left (right) HRS.

The two spectrometers are equipped with similar detector packages. Two vertical drift chambers, each with a U and V plane, provide kinematic reconstruction of charged particles. A segmented timing hodoscope and a gas Cherenkov counter (for e^+ identification) are used in the trigger. A two-layer lead glass calorimeter provides further offline particle identification. A single-paddle scintillator counter is used for timing alignment.

Data was collected with several triggers: single-arm triggers produced by the hodoscope in either arm, a raw coincidence trigger produced by a 40 -ns wide overlap between the hodoscope signals from the two arms, and a triple coincidence trigger of the previous coincidence signal and the Gas Cherenkov signal of the positron (right) arm. Single-arm trigger samples are used for optics and acceptance calibration, described below. The raw coincidence event sample, which is dominated by accidental $e^-\pi^+$ coincidences, is used to check the angular and momentum acceptance of the spectrometers. These $e^-\pi^+$ coincidences are largely rejected in the triple coincidence sample by the requirement of a Gas Cherenkov signal in the positron arm.

The reconstruction of e^+ and e^- trajectories at the target was calibrated using the "sieve slit method" (see [21, 25]). The "sieve slits" — removable Tungsten plates with a grid of holes drilled through at known positions — are inserted between the target and the septum magnet with a 1.131 GeV incident electron beam. A reconstruction correction matrix was obtained from e^- elastic scattering data taken with the sieve in place and using the ROOT package from [26], with care taken to avoid "focusing" systematics [27]. A kinematic

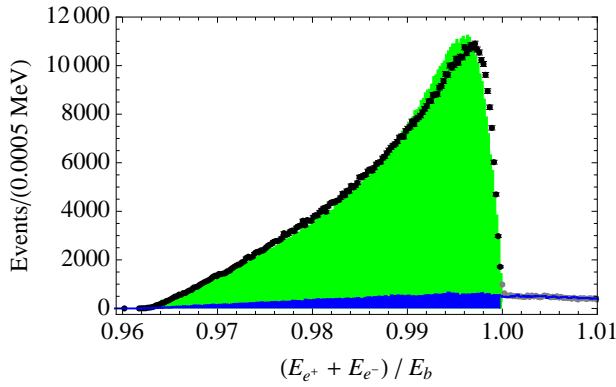


FIG. 3. The fraction of energy carried by the e^+e^- pair relative to the beam energy in the final coincidence sample (black, with error bars), the measured accidental component (blue), and Monte Carlo (green). Events rejected by the final kinematic selection $E(e^+) + E(e^-) < 2.261$ GeV are shown as gray dots, and the rejected accidental component by the blue line.

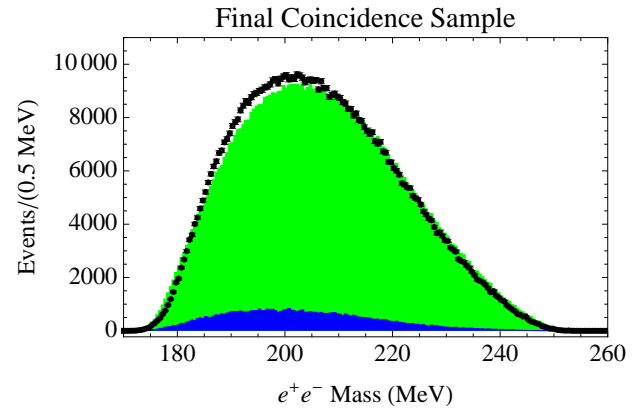


FIG. 4. The invariant mass spectrum of e^+e^- pair events in the final coincidence sample (black, with error bars), the measured accidental component (blue), and Monte Carlo (green).

selection was applied, so that only events within the boundary of the measured sieve holes are used in the final analysis.

The final coincidence event sample is selected from the triple coincidence sample by imposing a 12.5-ns timing window on the Gas Cherenkov and raw coincidence signals, requiring quality tracks in the vertical drift chambers of both arms, and the kinematic selection described above. Lastly, we demand that the sum of e^+ and e^- energies not exceed 2.261 GeV, the beam-energy threshold for true coincidence events (the effect of this cut on accidental coincidences is shown in Fig. 3). This final sample of 770,500 events consists almost entirely of true e^+e^- coincidence events with only 0.9% contamination by meson background, and 7.4% accidental e^+e^- coincidence events.

The experimental data was compared with a Monte Carlo calculation of the leading order QED trident process using MadGraph and MadEvent [28]. MadEvent was modified to account for nucleus-electron kinematics, and to use the nuclear elastic and inelastic form-factors in [29]. We neglect the effect of nuclear excitations on the kinematics in inelastic processes. Overall trident rates from the Monte Carlo for the test run configuration, accounting for acceptance, agree within a few percent with data. Likewise, the shapes of momentum and angular distributions agree within 5 – 10% differentially (see e.g. Fig. 3).

The performance of APEX depends critically on precise reconstruction of the invariant mass of e^+e^- pairs. The HRS momentum resolution is $O(10^{-4})$ for the kinematics of the APEX experiment. The mass resolution is instead controlled by three contributions to angular resolution: scattering of the e^+e^- inside the target, track measurement errors by the HRS detectors, and imperfections in the magnetic optics reconstruction matrix.

Multiple scattering in the target contributes 0.37 mrad to the vertical and horizontal angular resolutions for each particle.

Track measurement uncertainties contribute 0.28 (1.85) mrad to the horizontal (vertical) angular resolution in the left HRS and 0.44 (1.77) in the right HRS, determined from the observed sizes of the sieve slit holes in the data. Magnetic optics imperfections were found to contribute 0.10 (0.22) mrad to the horizontal (vertical) angular resolution. The resulting mass resolution was found to be 0.55 MeV from multiple scattering in the target, and 0.59 (0.56) MeV from horizontal (vertical) angular reconstruction and optics errors, giving a combined mass resolution of $\simeq 0.99$ MeV. Because calibration of the magnetic optics was performed using only e^- , and not e^+ , there is a possibility of additional aberrations in the positron arm. An upper limit for possible aberrations of 0.5 mrad was obtained from angular correlations in $H(e, e'p)$ experiments with the HRS and the calculations of the septa magnetic field. Accounting for these effects, we determine the combined mass resolution (rms) to be between 1.0 and 1.1 MeV. Finally, uncertainty in absolute angle between the two sieve slits introduces 1% uncertainty in the absolute mass scale but does not affect the mass resolution.

The starting point for the $A' \rightarrow e^+e^-$ search is the invariant mass distribution of the final coincident event sample, shown in Fig. 4. To avoid possible bias, the analysis code was tested and optimized on Monte Carlo and on a 10% sample of the coincident data.

A linear sideband analysis is not tenable in light of the high statistical sensitivity of the experiment and the appreciable curvature of the invariant mass distribution. Such an analysis would suffer from $O(1)$ systematic pulls, which can produce false positive signals or overstated sensitivity. Instead, a polynomial background model plus a Gaussian signal normalized to S events ($\sigma = 1.0$ MeV) is fit to a window bracketing each candidate A' mass. The uncertainty in the polynomial coefficients incorporates the systematic uncertainty in the shape of the background model. Based on extensive pseudo-experiment studies, a 7th-order polynomial fit over a 30.5 MeV window was found to achieve near-minimum un-

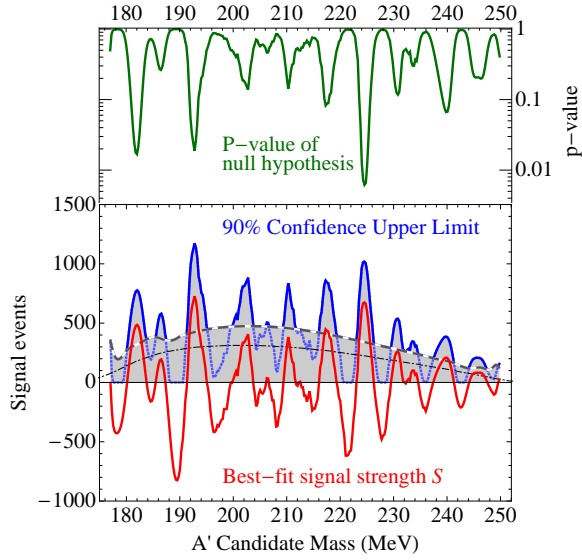


FIG. 5. **Top:** Background-model p -value versus A' mass. **Bottom:** Shaded gray region denotes 90% confidence, 50% power-constrained allowed region [30]. 90% confidence upper limit is shown in solid blue (dotted blue) when it is above (below) the expected limit (gray dashed). Red solid line denotes the best-fit for the number of signal events S . For comparison, thin dot-dashed line indicates contribution of statistical uncertainty to expected sensitivity, if background shape were known exactly.

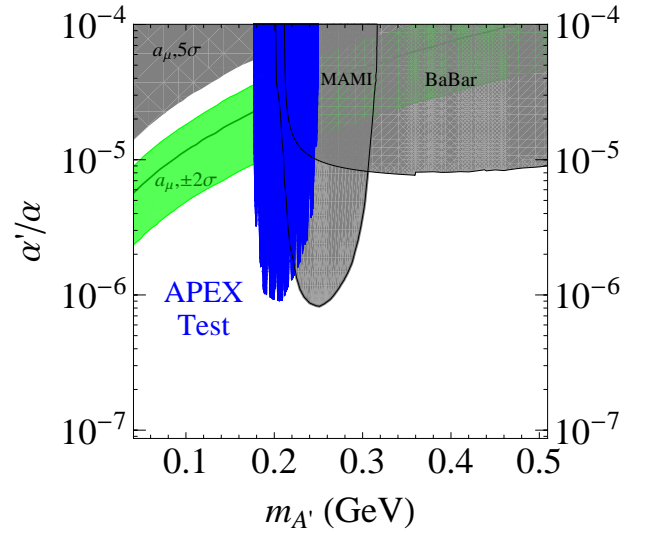


FIG. 6. 90% confidence upper limit on $\alpha'/\alpha \times Br(A' \rightarrow e^+e^-)$ versus A' mass for the APEX test run (blue). Shown in gray are existing constraints from the muon anomalous magnetic moment (5σ) [8], an approximate 90% confidence limit using BaBar results [3, 16, 31], and the 90% confidence limit reported by Mainz [23]. In the green 2σ region, the A' can explain a possible discrepancy between the calculated and measured muon anomalous magnetic moment [8]. The full APEX experiment will roughly cover the entire area of the plot.

certainty while maintaining a potential bias below 0.1σ across the mass spectrum. A symmetric window is used, except for candidate masses within 15 MeV of the upper or lower boundaries, for which a window of equal size touching the boundary is used. A binned profile likelihood ratio (PLR) is computed as a function of signal strength S at the candidate mass, using 0.05 MeV bins. The PLR is used to derive a 90%-confidence upper limit on the signal and the local p -value at $S = 0$ (i.e. the probability of a larger PLR arising from statistical fluctuations in the background-only model). We define the sensitivity of the search in terms of a 50% power-constraint [30], and do not regard a value of S as excluded if it is below this sensitivity threshold. This procedure is repeated in steps of 0.25 MeV. A *global* p -value, corrected for the “look-elsewhere effect”, (the fact that an excess of events *anywhere* in the range can mimic a signal), is derived from the lowest local p -value observed over the full mass range, and calibrated using pseudo-experiments.

We find no evidence of an A' signal. The p -value for the background model and upper bound on the absolute yield of $A' \rightarrow e^+e^-$ signal events (consistent with the data and background model) are shown in Fig. 5. The invariant-mass-dependent limit is $\simeq 200 - 500$ signal events at 90% confidence. The most significant excess, at 224.5 MeV, has a local p -value of 0.6%; the associated global p -value is 36% (i.e. in the absence of a signal, 36% of identically prepared experiments would observe a more significant effect due to fluctuations).

To translate the limit on signal events into an upper limit on the coupling α' with minimal systematic errors from acceptance and trigger efficiencies, we use a ratio method, normalizing A' production to the measured QED trident rate. The total QED trident background consists of *radiative* tridents (Fig. 1 (a)) and *Bethe-Heitler* tridents (Fig. 1 (b)) and their interference diagrams (we caution the reader that this nomenclature may not be standard). The A' signal and *radiative* trident fully differential cross sections are simply related (see [3]), and the ratio f of the radiative-only cross-section to the full trident cross-section can be reliably computed in Monte Carlo: f varies linearly from 0.21 to 0.25 across the APEX mass range, with a systematic uncertainty of 0.01, which dominates over Monte Carlo statistics and possible next-to-leading order QED effects. The 50% power-constrained limit on signal yield S_{max} and trident background yield $B_{\Delta m}$ in a mass window Δm determine an upper limit on α'/α ,

$$\left(\frac{\alpha'}{\alpha}\right)_{max} = \left(\frac{S_{max}/m_{A'}}{f B_{\Delta m}/\Delta m}\right) \times \left(\frac{2 N_{eff} \alpha}{3 \pi}\right), \quad (1)$$

where N_{eff} counts the number of available decay products (N_{eff} is 1 for $m_{A'} < 2m_\mu$, and increases to $\simeq 1.6$ at $m_{A'} \simeq 250$ MeV). The resulting limit, accounting in addition for contamination of the background by accidentals, is shown in Fig. 6.

In summary, the APEX test run data showed no significant signal of $A' \rightarrow e^+e^-$ electro-production in the mass range 175–250 MeV. We established an upper limit of $\alpha'/\alpha \simeq 10^{-6}$ at 90% confidence. All aspects of the full APEX experiment

outlined in [1] have been demonstrated to work. The full experiment will run at several beam energies, have improved mass coverage and resolution from a long multi-foil target, and acquire ~ 200 times more data than this test run, dramatically extending our knowledge of sub-GeV force.

The APEX collaboration thanks the JLab technical staff for their tremendous support during the brief test run. This work was supported by the U.S. Department of Energy. Jefferson Science Associates, LLC, operates Jefferson Lab for the U.S. DOE under U.S. DOE contract DE-AC05-06OR23177. This work was also supported in part by the U.S. Department of Energy under contract number DE-AC02-76SF00515 and by the National Science Foundation under Grant No. NSF PHY05-51164.

* rouven@slac.stanford.edu

† pschuster@perimeterinstitute.ca

‡ ntoro@perimeterinstitute.ca

§ bogdanw@jlab.org

- [1] R. Essig, P. Schuster, N. Toro, B. Wojtsekhowski, et al., JLab PAC 35 (2009).
- [2] R. Essig, P. Schuster, N. Toro, and B. Wojtsekhowski, JHEP **02**, 009 (2011), 1001.2557.
- [3] J. D. Bjorken, R. Essig, P. Schuster, and N. Toro, Phys. Rev. **D80**, 075018 (2009), 0906.0580.
- [4] B. Holdom, Phys. Lett. **B166**, 196 (1986).
- [5] R. Essig, P. Schuster, and N. Toro, Phys. Rev. **D80**, 015003 (2009), 0903.3941.
- [6] N. Arkani-Hamed, D. P. Finkbeiner, T. R. Slatyer, and N. Weiner, Phys. Rev. **D79**, 015014 (2009), 0810.0713.
- [7] M. Pospelov and A. Ritz, Phys. Lett. **B671**, 391 (2009), 0810.1502.

- [8] M. Pospelov (2008), 0811.1030.
- [9] N. Arkani-Hamed and N. Weiner, JHEP **12**, 104 (2008), 0810.0714.
- [10] C. Cheung, J. T. Ruderman, L.-T. Wang, and I. Yavin (2009), 0902.3246.
- [11] D. E. Morrissey, D. Poland, and K. M. Zurek (2009), 0904.2567.
- [12] B. Batell, M. Pospelov, and A. Ritz, Phys. Rev. **D80**, 095024 (2009), 0906.5614.
- [13] M. Freytsis, G. Ovanessian, and J. Thaler, JHEP **01**, 111 (2010), 0909.2862.
- [14] R. Essig, R. Harnik, J. Kaplan, and N. Toro, Phys. Rev. **D82**, 113008 (2010), 1008.0636.
- [15] B. Batell, M. Pospelov, and A. Ritz (2009), 0903.0363.
- [16] M. Reece and L.-T. Wang (2009), 0904.1743.
- [17] B. Aubert et al. (BABAR) (2009), 0908.2821.
- [18] KLOE collaboration, e.g. <http://www.roma1.infn.it/discrete10/>.
- [19] V. M. Abazov et al. (D0), Phys. Rev. Lett. **103**, 081802 (2009), 0905.1478.
- [20] V. M. Abazov et al. (D0), Phys. Rev. Lett. **105**, 211802 (2010), 1008.3356.
- [21] J. Alcorn et al., Nucl. Instrum. Meth. **A522**, 294 (2004).
- [22] e.g. <http://conferences.jlab.org/hps2011/program.html>.
- [23] H. Merkel et al. (2011), 1101.4091.
- [24] e.g. http://www.desy.de/~bechtel/talks/PBe_HIPS_shortoverview.100630.pdf.
- [25] E. Offermann, C. D. Jager, and H. D. Vries, Nucl. Instrum. Meth. **262**, 298 (1987).
- [26] I. Antcheva et al., Computer Physics Communications **180**, 2499 (2009).
- [27] T. Veit, J. Friedrich, and E. Offermann, Nucl. Instrum. Meth. **336**, 572 (1993).
- [28] J. Alwall et al., JHEP **09**, 028 (2007), 0706.2334.
- [29] K. J. Kim and Y.-S. Tsai, Phys. Rev. **D8**, 3109 (1973).
- [30] G. Cowan, K. Cranmer, E. Gross, and O. Vitells (2011), 1105.3166.
- [31] B. Aubert et al. (BABAR) (2009), 0902.2176.